

A GCN-Attention Model for Precision Irrigation Evaluation

Ying Huang and Meng Liu

Abstract—The challenges of traditional quantitative irrigation methods cannot adapt to the dynamic actual soil moisture content and meteorological changes, and the existing methods based on soil moisture thresholds cannot fully solve the problems of hysteresis and adaptability, lack comprehensive consideration of meteorological factors and growth dynamics, and fail to consider the subtle sensitivity to soil moisture changes and processing efficiency limitations. To address the above challenges, we propose UFO-GCN-SPANet, a novel and computationally efficient architecture specifically designed for resource-constrained precision agriculture. Its core innovation lies in the cascaded integration of: (1) a linear-complexity Unit Force Operated Vision Transformer (UFO-ViT) that replaces quadratic self-attention with matrix associativity and cross-normalization for efficient global spatio-temporal feature extraction; (2) Graph Convolutional Networks (GCNs) for modeling spatial dependencies; and (3) a Salient Positions-based Attention Network (SPANet) employing a novel Significant Position Selection (SPS) algorithm to dynamically focus computation on the most informative contextual features, drastically reducing complexity while enhancing discriminative power. This unique combination directly addresses the critical challenges of computational efficiency and effective context modeling in real-world irrigation systems. Experimental results show that the proposed method outperforms traditional GNN models such as SAGEConv with 12 standard time series forecasting methods in key metrics, including accuracy, precision, recall, and F1-Score.

Index Terms—Precision Agriculture, Soil Moisture Prediction, Machine learning

Original Research Paper
DOI 10.53314/ELS2529070H

Manuscript received on May 17th, 2025. Received in revised form on August 26th, 2025. Accepted for publication on September 17th, 2025.

Ying Huang is with the Faculty of School of Automotive and Information Engineering, Guangxi Eco-engineering Vocational and Technical College, Liuzhou Guangxi, P.R. China. At the same time, he is pursuing a doctoral degree at Wuhan University. (e-mail: huangying800816@163.com).

Meng Liu is with the Faculty of School of Automotive and Information Engineering, Guangxi Eco-engineering Vocational and Technical College, Liuzhou Guangxi, P.R. China (corresponding author, e-mail: 517273947@qq.com).

This paper was supported by the Talent Introduction Scientific Research Project (NO.GXSTKYZX202406002) of Guangxi Ecological Engineering Vocational and Technical College, the first phase of the training project of famous teachers (craftsmen), and the project construction project of famous master studios.

I. INTRODUCTION

THE soil moisture content plays a significant impact on various aspects of agriculture and water resource management, affecting crop growth, irrigation efficiency, yields, and health. Insufficient soil moisture would impair crop growth, excessive soil water would lead to root diseases, affecting crop health. Precise irrigation decision is a complex task involving multiple factors, requiring consideration of soil water content, soil temperature, and various weather conditions, which involves technologies such as sensor technology, IoT (Internet of Things), artificial intelligence, and data analytics techniques.

A smart irrigation system is an intelligent management platform designed to optimize crop growth conditions by precisely controlling the amount of water applied, increasing water resource utilization efficiency, and mainly composed of sensing layer, communication layer, data layer, model layer, and decision layer, as shown in Fig. 1.

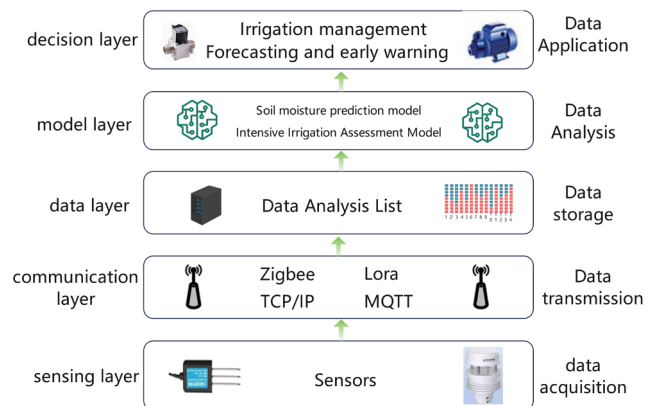


Fig. 1. Block Diagram of Precision Irrigation System Components

The sensing layer primarily consists of soil parameter sensors (e.g., moisture and temperature) and meteorological station sensors (e.g., temperature, humidity, and rain quantity), which collect data from the field and convert it into a signal for real-time status information to provide. The communication layer utilizes wireless communication technology to process data collected from sensors, sending to the central processing system. The data layer stores raw data and dealt with information, supporting model layer and decision layer's computation and analysis. The model layer includes soil moisture prediction model and precipitation evaluation model, providing scientific decision-making based on the model layer's results. The decision layer generates irrigation decisions based on the results

from the model layer, determining when to water, how much to water, and how to water, using real-time data and predictive models to automatically adjust the irrigation plan and send an instruction for controlling the irrigation controller, valves, and pumps on the hardware devices, enabling the operation of the irrigation system.

In the system, information flow and control flow are clearly illustrated in Fig. 2. Lora nodes collect soil parameters and weather parameters via 3G/4G/GPRS technologies and transmit them to the cloud server. Users can interact with the terminal interface to retrieve and administer data. The user controller processes and models the gathered information, formulates the irrigation decision plan, and distributes results through a network to Lora nodes for control of the electric valves that regulate the irrigation machinery.

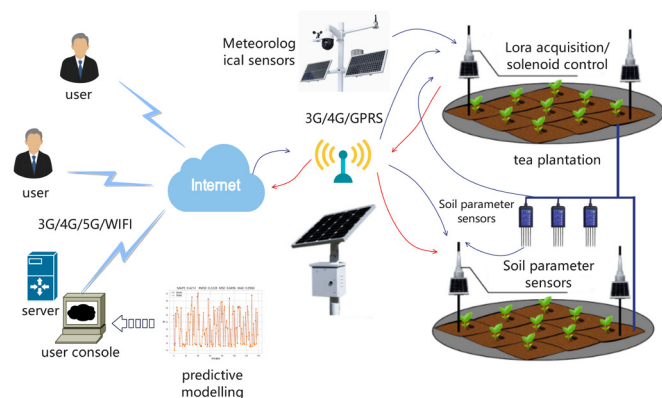


Fig. 2. Schematic diagram of data and information flow of precision irrigation system

The ecological economy and economic benefits of the tea industry are closely connected with irrigation efficiency. The growth of tea trees is highly sensitive to soil moisture content, and changes in soil moisture content directly affect the yield and quality of tea leaves. The water demand of tea trees exhibits significant seasonal variation. The water requirement of tea trees shows notable differences during various growth stages, with higher demand during the seedling and growth stages. Moderately controlling irrigation before the harvest period can increase the quality and yield of tea leaves, while irrigation should be reduced in winter to prevent root frost damage. This dynamic water demand places higher demands on the real-time monitoring accuracy of soil moisture content. Additionally, tea plantations are situated in hilly and mountainous areas, where the complex terrain leads to differentiated soil moisture content at different slopes and altitudes. These unique topographical conditions impose higher requirements for the design and implementation of irrigation systems, making it difficult for traditional empirical irrigation methods to cope with the moisture disparities caused by complex terrain, which can easily lead to localized water shortages or flooding. The unique microclimate conditions also directly impact the water supply and irrigation needs of the tea garden, adding to the difficulty of irrigation.

Accurately predicting soil moisture is essential for providing systematic irrigation guidance and optimizing water re-

sources. Therefore, precise irrigation requires the use of accurate irrigation decision models that may be influenced by soil moisture, crop needs, and meteorological conditions. This demands a irrigation management system that can accurately detect and address these non-linear characteristics. The variability in soil moisture across different regions also necessitates that efficient irrigation handles localized monitoring and differential management of soil moisture. On the other hand, quantitative irrigation with fixed schedule is typically initiated by limiting soil moisture levels, such as when there are drought conditions. However, deciding whether a field is dry or need watering requires personal experience and effort during irrigation. Moreover, the difficulty in precise gauging irrigation duration and quantity, coupled with the variability across fields, leads to significant water waste issues.

The research and application of integrated water-saving techniques, such as drip irrigation and water-fertilizer integration, are still in the research stage and demonstration phase. Due to insufficient technical maturity, the fields in data collection and irrigation decisions will continue to face challenges, while also facing a gap with other technologies tree combinations. The precision of the methods for irrigation has room for significant research space regarding the application in tea trees. Deep learning is continuously advancing, making its modeling method prominent in the field of irrigation precise planning. The study on machine learning for tea tree irrigation decision-making prediction and assessment is deficient. In this manuscript, we propose the novel UFO-GCN-SPANet framework maintains compatibility with mainstream IoT irrigation platforms through standardized data interfaces and control protocols. As illustrated in Fig. 1 and Fig. 2, the model layer can directly process sensor data from existing monitoring systems and generate irrigation commands compatible with commercial controllers, which feature:

The first application of UFO-ViT's linearized self-attention mechanism ($O(N)$ complexity) in precision agriculture, effectively overcoming the computational bottleneck of standard Transformers ($O(N^2)$) for modeling long-range dependencies in sensor network data.

The introduction of SPANet with the innovative SPS algorithm into the irrigation evaluation domain. SPS actively selects only the top-k salient positions for attention computation, achieving significant reductions in computational cost and memory footprint while enhancing model focus on critical contextual information and node-level interactions.

A purpose-built cascaded architecture (UFO-ViT \rightarrow GCN \rightarrow SPANet) designed to progressively learn rich global features, incorporate spatial topology, and perform focused context refinement, specifically optimized for the efficiency demands and dynamic nature of resource-limited agricultural environments.

Comprehensive experimental validation and ablation studies demonstrate the substantial individual and synergistic contributions of each proposed component (UFO-ViT, SPANet) to the overall model's superior accuracy and efficiency.

II. RELATED WORKS

Machine learning algorithms are increasingly used in water resources prediction, and scholars have made significant advancements. Puspaningrum et al. proposed a machine learning algorithm for irrigation prediction, which is capable of accurately predicting irrigation using classification algorithms such as support vector machine, k-nearest neighbors, Plain Bayes, Random Forest, and Decision Tree in the method [1].

Priya et al. integrated IoT technology and machine learning algorithms with precision agriculture by using sensors to collect data such as temperature, humidity, soil moisture, and water level, and used different machine learning models including support vector machine, decision tree, random forest, and plain Bayes to predict crop water requirement and control the operation of pumps based on the prediction results to optimise irrigation management [2].

Filgueiras proposed a methodology to predict water management parameters based on Vegetation Indices (VIs) and regression algorithms, where Random Forests, Cubic Regression, and Gradient Boosters were used for validation of the data to fulfil the need for fully remote irrigation management [3].

Abioye et al. focused on IoT-based monitoring and data-driven modelling of drip irrigation system for mustard leaf cultivation and proposed an improved monitoring and data-driven model for monitoring the dynamics of parameters affecting the irrigation of rapeseed leaf plants [4].

Narakala et al. constructed a Crop Water Stress Index (CWSI) model, which takes three parameters as inputs such as relative humidity, air temperature, and canopy temperature, and various machine learning methods such as multi-layer perceptron, random forests, and decision trees were used to evaluate the CWSI model, and all of them showed good performance [5].

The study by Bwambale et al. demonstrated the great potential of machine learning in improving the accuracy of irrigation management and also proposed a data-driven model predictive control approach for precision irrigation, highlighting the importance of accurate predictive modelling for optimising water use [6].

In order to be able to avoid water wastage, Bhoi et al. used machine learning and IoT techniques to build a smart irrigation recommendation system that combines various machine learning based support vector regression and KNN classifier models to achieve efficient water use and reduce human intervention [7].

Vianny et al. proposed a hybrid model of an irrigation system using IoT components to collect information on soil moisture, soil temperature, weather conditions and environmental conditions, incorporating algorithms such as KNN, gradient boosting based trees, long and short-term memory and Spearman rank correlation to optimise demand and thus reduce energy consumption [8].

The development of smart irrigation systems has been the focus of recent research efforts. Campos et al. proposed the Smart and Green framework to provide data monitoring, preprocessing, fusion, synchronisation, storage and irrigation

management services for smart irrigation and to enrich these services by predicting soil moisture [9].

Liao et al. developed an intelligent irrigation system based on real-time soil moisture data, emphasising the importance of water-saving irrigation scheduling and the development of efficient automated irrigation systems [10].

Choi et al. emphasized the need for a more accurate transpiration model for tomato cultivation in order to achieve precise irrigation control in greenhouse soilless culture [11].

Similarly, Jo et al. aimed to develop a transpiration model for precise control of tomato irrigation under various environmental conditions in greenhouses. These studies highlight the importance of accurate transpiration modelling for efficient irrigation strategies [12].

In the field of precision irrigation, Chen et al. designed and implemented an intelligent irrigation robot to solve the problems of poor mobility, inaccuracy and high price in agricultural irrigation systems. The robot achieved precision irrigation through an improved irrigation path planning algorithm based on Bayesian theory [13].

In addition, Wu et al. explored the use of Ground Penetrating Radar (GPR) full-wave inversion to map soil moisture in a potato field in furrowed mound terrain, focusing on the effect of soil surface in furrowed mound terrain on GPR measurements for mapping soil moisture [14].

Abera et al. used extracted Soil-Adjusted Vegetation Index (SAVI) image greenness to identify irrigated cropland and used more precise irrigation techniques to minimize water losses by calculating the irrigation water requirement of the major crops grown under irrigation and determined using estimated irrigated area of the watershed [15]. These research methods and techniques provided the methodology and ideas to this project to study the precision irrigation techniques for tea trees.

Despite the success of research in precision irrigation, there are still multiple challenges to overcome. The variability of soil moisture content in different regions requires greater flexibility and adaptability of irrigation systems. The maturity and application scope of the technology needs to be improved, especially in the accuracy of data collection and irrigation decision making. Future research should focus on the integration and application of multiple technologies to promote the popularization and application of smart irrigation technologies and provide technical support for sustainable agricultural development.

III. RELATED TECHNOLOGIES

A. Graph Convolutional Network

Graph Convolutional Networks (GCNNs) are designed for modeling graph-structured data and can effectively capture complex relationships between nodes [16]-[17].

Given a graph $G = \{C, E\}$, let the node feature matrix be $X \in R^{N \times D}$, the adjacency matrix A and the degree matrix D . The output $Z \in R^{N \times F}$, with L layers. The propagation at each layer is defined as equation (1):

$$H^{(l+1)} = f(H^l, A) \quad (1)$$

where, $H^{(0)} = X, H^{(L)} = Z$, the number of layers of the network denoted L , the model selection and parameter approach will vary depending on the function $f(\cdot, \cdot)$, which $f(\cdot, \cdot)$ is the propagation rule.

So, a basic propagation rule is defined as equation (2):

$$f(H^{(l)}, A) = \sigma(AH^{(l)}W^{(l)}) \quad (2)$$

where $W^{(l)}$ denotes the weight matrix of the l th layer, which is used to map the l th layer features to the $l + 1$ th layer, and $\sigma(\cdot)$ denotes the nonlinear activation function.

To stabilize the model, the adjacency matrix is typically normalized (adding self-loops followed by symmetric normalization), as shown in equation (3):

$$\hat{A} = D^{-\frac{1}{2}}AD^{-\frac{1}{2}} \quad (3)$$

The final standard propagation rule is then given by (4):

$$f(H^{(l)}, A) = \sigma(\hat{D}^{-\frac{1}{2}}\hat{A}\hat{D}^{-\frac{1}{2}}H^{(l)}W^{(l)}) \quad (4)$$

where $D^{-\frac{1}{2}}$ represents the square root of the inverse of the degree matrix, $\hat{A} = A + I$ is the unit matrix and \hat{D} is the degree matrix of \hat{A}

The GCN-based soil moisture prediction method follows these key steps:

1. Sampling: Randomly select neighboring nodes (guided by a predefined strategy to limit computational load).
2. Aggregation: Combine neighbor features (via mean/max/pooling) to represent the target node, capturing local graph structure.
3. Update: Transform aggregated features using a learnable weight matrix to enhance model expressiveness.
4. Propagation: Iteratively repeat sampling-aggregation-update until all nodes are processed, yielding updated node features.

B. Unit Force Operated Vision Transformer

The Transformer excels in vision and NLP tasks but faces three key challenges:

- 1) High Complexity: Self-attention scales quadratically with sequence length, increasing training time and resource demands.
- 2) Data Hunger: Requires large datasets to match CNN performance in low-data regimes.
- 3) Static Modeling: Struggles with spatio-temporal dynamics (e.g., video analysis).

To solve this problem, Unit Force Operated UFO-ViT (Unit Force Operated Vision Transformer) replaces softmax with cross-normalization (XNorm), reducing complexity while preserving performance [18]. Its architecture includes: normalisation layer, UFO model, convolutional layer and MLP model, the specific model is shown in Fig. 3.

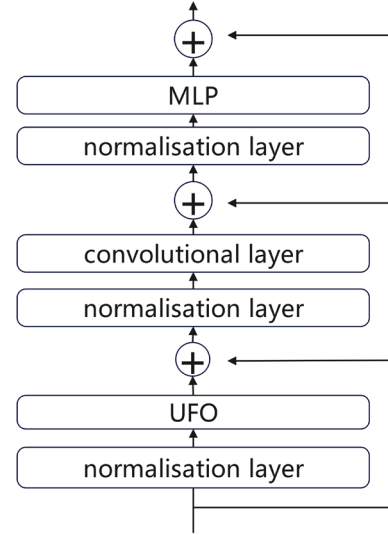


Fig. 3. Structure of the UFO-ViT model

For the attention mechanism A in the Transformer model is computed via equation (5), in which Q , K and V defined in equations (6), (7) and (8), are first obtained by linearly projecting the input sequence:

$$A = \text{softmax}\left(\frac{K^T Q}{\sqrt{d}}\right) \quad (5)$$

where:

$$Q = XW_Q \quad (6)$$

$$K = XW_K \quad (7)$$

$$V = XW_V \quad (8)$$

X denotes is the input feature vector, Q , K and V denote the query vector, key vector and value vector, W_Q , W_K and W_V weight matrices, d is the dimension of the input feature vector.

The nonlinear nature of softmax makes it impossible to decompose the result into $O(N \times h + h \times N)$. To solve this problem, the self-attention mechanism model is allowed to multiply first, eliminating the original softmax. but this method leads to performance degradation. Therefore, a cross-normalisation method (denoted as XNorm) is used, as defined by (9) and (10):

$$A(\mathbf{x}) = \text{XN}_{\text{dim=filter}}(Q)(\text{XN}_{\text{dim=space}}(K^T V)) \quad (9)$$

$$\text{XN}(\mathbf{a}) = \frac{\gamma \mathbf{a}}{\sqrt{\sum_{i=0}^h \|\mathbf{a}\|^2}} \quad (10)$$

where: γ denotes the learnable parameter, h denotes the embedding dimension, which is an L2 paradigm that applies not only to the spatial dimension of $K^T V$, but also to the channel dimension of Q .

Using the law of union, first let V and K be multiplied together and then multiplied with Q . The final result is linear with respect to n . The complexity of the two multiplications is $O(hNd)$. Since the complexity of the two multiplications is $O(hNd)$, the final result also has a linear relationship with n . The complexity of the two multiplications is $O(hNd)$. This is shown in Fig. 4.

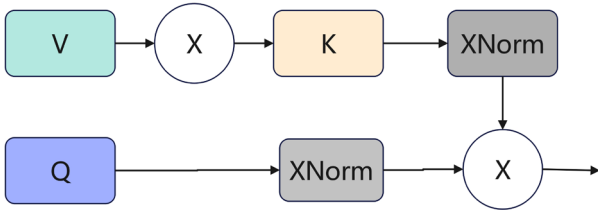


Fig. 4. Block diagram of the linearisation of the attention mechanism

C. Salient Positions-based Attention Schemer

Attention mechanisms, given their capacity to efficiently manage long-range dependencies in input sequences, are highly effective for tasks such as text and speech processing and have garnered substantial attention. As the global dependencies among input features increase, the demand for computational resources and memory correspondingly rises. While the attention mechanism can gather information globally, not all such information is beneficial for context modeling, potentially leading to performance degradation. To address this, SPANet introduces a method that computes attention solely on salient locations (a limited number of keypoints). This approach not only conserves a significant amount of computational resources and memory but also extracts useful information from the input feature maps, thereby enhancing prediction performance [19].

The structure of SPANet is shown in Fig. 5.

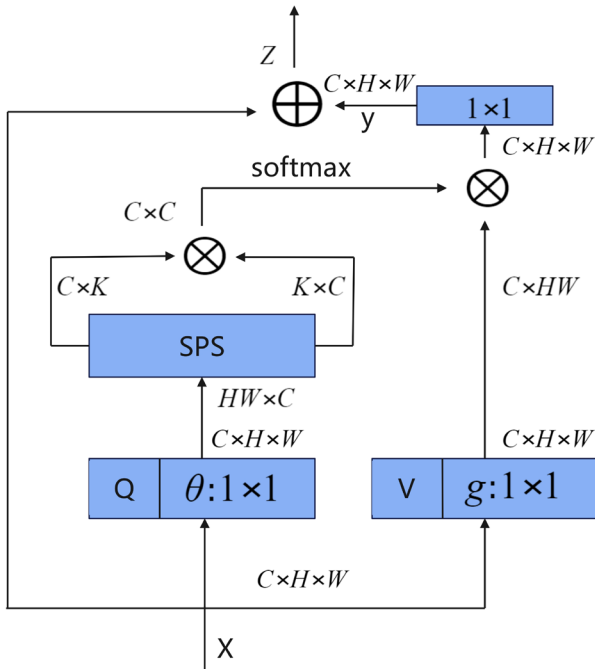


Fig. 5. SPANet structure

The input X is first transformed by a 1×1 convolution to yield Q and V , respectively. Q is then processed by the SPS algorithm, which extracts the top- k significant query-key matrices according to equations (11) - (13).

$$Q = \theta(x) \quad (11)$$

$$V = g(x) \quad (12)$$

$$K = S(Q) \quad (13)$$

The affinity matrix A is computed with a softmax over the top- k significant locations, as given in equation (14). And is multiplied by V to yield the output Y , as given by (15):

$$A = \text{softmax}\left(\frac{K^T K}{c}\right) \quad (14)$$

$$Y = VA \quad (15)$$

After a 1×1 convolution, Y is finally added back to the original input X .

In the SPS algorithm, positive context information is extracted when modelling global dependencies, i.e., attentional computation is performed at salient locations, which reduces the complexity of the computational procedure. The SPS algorithm can be described as:

1. input query key Q of dimension $[c, h \times w]$, hyperparameter k value
2. Calculate the square power of $Q^T Q$ based on the channel dimension
3. Sum $Q^T Q$ to get Q_{pow}
4. sort by largest to smallest, take the first k values, and add index
5. return $K = Q(c, \text{index})$

IV. METHODS FOR PRECISION IRRIGATION EVALUATION

A. General structure

Accurate prediction of soil water content is an important basis for providing scientific irrigation guidance and optimizing water use. Graph conventional neural networks may be unable to adequately capture all the complex relationships in the graph, while traditional attention mechanisms, although effective in dealing with long-distance dependencies in the input sequences, are deficient in capturing information about the spatio-temporal dynamics. As the global dependencies of the input features increase, the complexity and training cost of the model also rise, and the demand for computational resources and memory continues to increase. To address these issues, this manuscript proposes a graph neural network refined irrigation prediction method based on a fusion attention mechanism (UFO-GCN-SPANet) to overcome the inefficiency of graph neural networks in processing complex data, the insufficient global feature extraction, the non-enrichment of feature representations, and the multimodal data fusion problem, which firstly introduces a unit-forcing operation visual Transformer self-attention mechanism (UFO-ViT). The method firstly introduces the unit forced operation visual Transformer self-attention scheme (UFO-ViT), which significantly reduces the computational resources and generates high-quality feature representations to provide rich information for the graph neural network by using its linear complexity design, and then introduces the Salient Positions-based Attention Scheme (SPANet) after the graph neural network to provide rich information for the graph neural network by means of the Salient Positions Selection (SPS) to select only a limited number of salient points for attention graph computation, which not only reduces the computational complexity and memory requirements, but also improves

the accuracy of image classification by extracting positive contextual information through selecting salient positions. The extraction of high-quality global features by UFO-ViT, graph structure information by GCN modelling, and positive context information by SPANet makes the whole network more efficient in processing large scale data and reduces computational resources and memory requirements. This method has significant practical application value in the field of agriculture, which can significantly improve the scientific and accuracy of irrigation strategies. The overall structure of the algorithm is illustrated in Fig. 6.

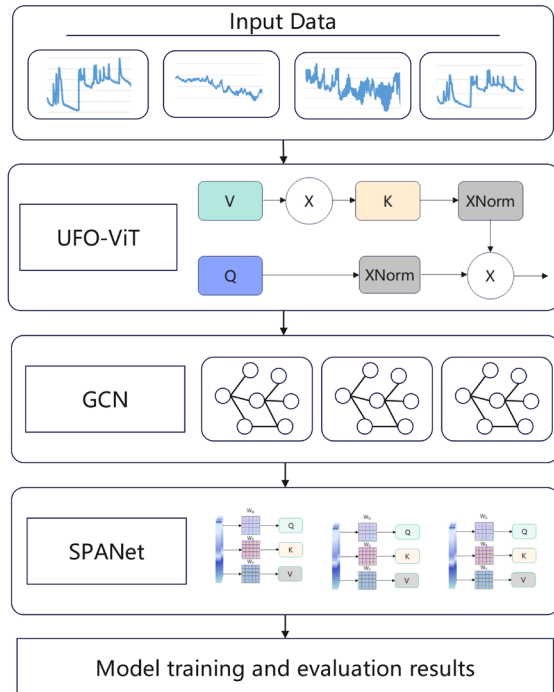


Fig. 6. Structure of graph neural network algorithm incorporating attention mechanism

The novelty and effectiveness of UFO-GCN-SPANet stem primarily from two key innovative components and their synergistic integration within the cascade.

UFO-ViT: Revolutionizing Efficiency in Global Modeling

Standard Transformer self-attention, with its $O(N^2)$ computational complexity and memory requirements, becomes prohibitively expensive for processing the potentially long time-series and numerous nodes in agricultural sensor networks, hindering real-time deployment on edge devices. UFO-ViT fundamentally rethinks attention by leveraging matrix multiplication associativity and introducing Cross Normalization (XNorm). This allows it to completely eliminate the computationally intensive $\text{softmax}(QK^T)$ operation central to standard Transformers. The resulting linear complexity ($O(N)$) enables UFO-ViT to efficiently capture complex long-range spatio-temporal dependencies across the entire sensor network without sacrificing representational power. This breakthrough in efficiency is crucial for practical applicability in resource-constrained precision irrigation systems.

SPANet: Selective Attention for Efficiency and Focus

While attention is powerful, computing interactions between all positions is often redundant and computationally wasteful. Noise and irrelevant variations in sensor data can dilute the effectiveness of standard attention. SPANet incorporates SPS algorithm dynamically identifies the top-k most significant positions (or nodes) based on the input features, slashing computational cost and memory usage, particularly beneficial for large graphs or long sequences. By focusing computation and modeling capacity on the most informative contextual interactions, SPANet effectively filters out noise and amplifies relevant signals, leading to more robust and discriminative node representations. This selective focus is a distinct advantage over standard, unselective attention mechanisms.

The sequential flow UFO-ViT (Efficient Global) \rightarrow GCN (Spatial Structure) \rightarrow SPANet (Focused Context Refinement) is carefully designed. UFO-ViT provides rich, efficient input features. GCN injects explicit spatial relationships. SPANet then performs localized, context-aware enhancement based on the graph-informed features, maximizing the utility of the selective attention. This holistic design directly targets the intertwined challenges of efficiency, global context, spatial structure, and relevant local interaction in precise irrigation evaluation.

B. Data processing and classification methods

In order to achieve dynamic and intensive irrigation, the soil water content variable servers as a basis for the study, and the data objects of the study are pre-processed. In order to make better decisions on precision irrigation, the soil water content can be classified as 'low', 'medium', 'high', or several types for specific purposes. In this section, the data are classified from 0 to 1, and the data are classified into three types of 'low,' 'medium,' and 'high,' or several types for specific uses, which can be classified into different irrigation levels to form a dynamic irrigation management model. In this section, the data are split into 10 equal parts from 0 to 1, in which interval they are classified, e.g., 0-0.1 is classified as the first class, 0.1-0.2 is classified as the second class, and so on.

1) Normalization. Each column of the input is first normalized to the range $[0, 1]$ via equation (16):

$$x' = \frac{x - \min(x)}{\max(x) - \min(x)} \quad (16)$$

where x is the input data, $\min(x)$ represents the minimum value of the data and $\max(x)$ represents the maximum value of the data.

2) create dictionary labels that map the index of each category to a key in the form of a string.

3) Produce the dataset. Obtain a list of paths and labels based on the dictionary of labels and the number of categories. The last column in the dataset is invoked as a random number, which is sorted according to the set number of categories to get the corresponding label.

C. Process for precision irrigation evaluation

1) Data classification. According to the data classification division method, the soil water content is divided into 10

classes, labelled 0-9 in order, and each class corresponds to a unique irrigation strategy.

2) feature mapping. After data transformation to get x , its data shape is $(batch_size, dim)$, $batch_size$ represents the number of samples extracted from the training data each time, dim represents the number of features. A linear transformation is performed by linear to map the input features from dim to a higher dimension ($dimh$).

3) Data reshaping. The obtained data $((batch_size, dimh)$ is reshaped into $(batch_size, time_steps, nodes, 2)$ to fit the input format of graph convolutional network.

4) Graph Convolution Processing. The reshaped data is further reshaped into $(batch_size * 10, 4, 2)$ and fed into the GCN model. Attention transformation is made on the input features using UFOAttention and attention weighted features are computed. Calculate support features support with shape $(batch_size * time_steps, nodes, out_features)$. Graph convolution operation is performed using the adjacency matrix adj and the output shape is $(batch_size * time_steps, nodes, out_features)$. $out_features$ represent the number of output features. The output data is further processed by SPABlock by batch normalisation layer $BatchNorm1d$ and the shape becomes $(batch_size * 10, nhid)$, where $nhid$ represents the hidden layer feature dimension.

5) Activation and reshaping. Data is reshaped to $(batch_size, nhid, 10)$ by ReLU activation function with transpose operation.

6) Feature Spreading. Reshape the processed obtained data into $(batch_size, time_steps, -1)$ and transpose it into $(batch_size, -1, time_steps)$, spreading it to fit the input of the linear classifier.

7) linear classification. Map the spread features to the number of categories by $linear2$, the output shape is $(batch_size, num_classes)$, which represents the category prediction for each sample.

8) Output results. The final output is the category prediction for each sample in the shape of $(batch_size, num_classes)$.

The labels of the data labels are an essential part of the training process used to calculate the loss, but they are not directly involved in the forward propagation of the model. In the training loop, the output of the model is to be sent into the loss function along with the labels, and the loss function calculates the difference between the predicted output and the true labels to generate a loss value. The calculated loss value is used for back propagation to update the parameters of the model to minimise the loss. The model is learnt by adjusting the parameters to make the forecast output closer to the labels.

V. EXPERIMENTS AND ANALYSES

A. Experimental evaluation indicators and settings

1) Experimental Data

The experimental dataset consists of real-world field sensor data collected from Liucheng County state-owned Fuhu Overseas Chinese Farm Tea Factory, a commercial tea plantation located in Liuzhou Guangxi Province, China. A wireless sensor

network (WSN) was deployed across the plantation, comprising nodes equipped with sensors for measuring Environmental parameters, soil temperature (ST), soil electrical conductivity (SEC), and soil moisture content (SMC). The environmental parameter collection uses the integrated environmental monitor of Guangzhou Hairui Intelligent Technology Co., Ltd., which can realize the collection of seven elements of air temperature, air humidity, illumination, air pressure, rainfall, wind speed and wind direction. And ST, SEC and SMC are completed by the MEC20 trinity sensor of Dalian Zheqin Technology Co., Ltd. Data was logged at intervals of 15 minutes.

The raw data collection spanned from August 10, 2020, to March 27, 2021, yielding a total of 31,464 raw data records. To analyze and utilize this data more effectively, missing values were addressed using linear interpolation for short gaps; records with consecutive missing values exceeding 1 hour were removed. 700 datasets were obtained by processing missing values during the preprocessing stage. Each dataset sample comprises the synchronized readings of the aforementioned environmental and soil parameters as input features, with the corresponding SMC serving as the target output variable for prediction and subsequent classification.

2) Evaluation Metrics

The model was trained and assessed using Accuracy (A_{cc}), Precision (P_{pv}) and Recall (R_{ec}) and F1-Score, whose explicit definitions are given in equations (17)–(20).

$$A_{cc} = \frac{TP+TN}{TP+TN+FP+FN} \quad (17)$$

$$P_{pv} = \frac{TP}{TP+FP} \quad (18)$$

$$R_{ec} = \frac{TP}{TP+FN} \quad (19)$$

$$F1_Score = 2 \times \frac{P_{pv} \times R_{ec}}{P_{pv} + R_{ec}} \quad (20)$$

where TP denotes True Positive, i.e., the number of samples correctly predicted by the model as positive samples; TN denotes True Negative, i.e., the number of samples correctly predicted by the model as negative samples; FP denotes False Positive, i.e., the number of samples incorrectly predicted by the model as positive samples; and FN denotes False Negative (False Negative), i.e., the number of samples that the model incorrectly predicts as negative.

3) Experimental platforms

The MSI Punch Tank GL65 laptop with Intel(R) Core (TM) i7-9750H CPU @ 2.60GHz, 2.59 GHz and 32GB of RAM is used for this experiment. The software environment for the experiment is under Windows 11 system platform using Anaconda development tools and pytorch_ geometric framework to perform the experiments.

4) Experimental settings

In the SPANet attention mechanism module, the main parameters are the number of channels in the input feature map in channels, the value of which depends on the input data; the number of ‘most important’ elements selected at each position of the feature map $k = 4$ (depending on the dimensionality of the input data); and the flag bit to set the value of k adaptively.

adaptive (set to False), if adaptive is True, then k will be calculated based on N (the spatial dimensionality of the feature map) and reductions, the default value is 16; whether to use k as a parameter for learning (set to False); the mode for calculating the spatial attention, the default is 'pow', i.e., the square calculation used to calculate the importance of the data.

The main parameters in the UFOAttention module are: the output dimension of the model d_{model} , the dimensions of the query vectors (queries) and key vectors (keys) d_k , the dimension of the value vectors (values) d_v the number of main headers h . According to the actual needs of the experiment, they are all set to 2.

The main data in the GCN module of the graphical convolutional neural network are: the number of output classification categories $\text{num_classes}=10$; the input data dimension in_features (depending on the input data), the output data dimension out_features (depending on the input data), the bias flag bias (set to True), and the number of hidden layers $\text{nhid}=16$.

B. Algorithms for comparison

On the collected soil data, the proposed method is compared with other models in an experiment. The main models compared are SAGEConv [20], GCNConv [21], GATConv [22], GraphConv [23], FeaStConv [24], ARMAConv [25], SGConv [26], GATv2Conv [27], TransformerConv [28], SSGConv [29], GENConv [30] and SuperGATConv [31].

C. Experimental results and analyses

1) Prediction performance experiment of the algorithm

The prediction performance experiments of the proposed method are conducted on the collected dataset of soil water content.

The confusion matrix of the UFO-GCN-SPANet model run is shown in Fig. 7.

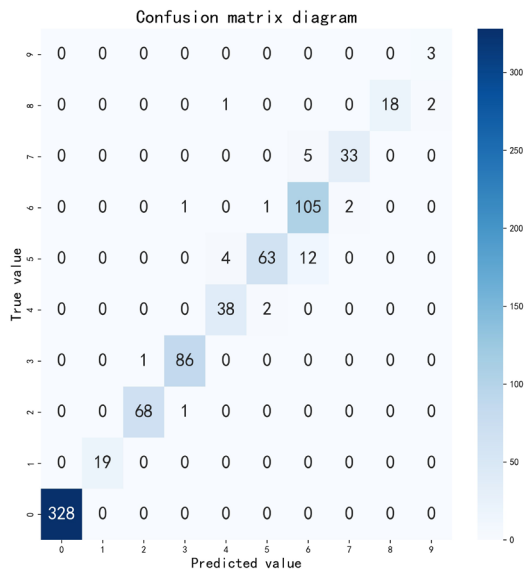


Fig. 7. UFO-GCN-SPANet model prediction confusion matrix

Since multiple classifications are involved, this method calculates the precision, recall and F1 values for each category separately, and then averages them as the final indicator value for the classification. In Table I, the precision, recall and F1 values for each category in the model prediction.

TABLE I
EVALUATION INDICATOR RESULTS BY CATEGORY

Class	P_{pv}	R_{ec}	F1_Score
Class 0	1.0000	1.0000	1.0000
Class 1	1.0000	1.0000	1.0000
Class 2	0.9855	0.9855	0.9855
Class 3	0.9773	0.9885	0.9829
Class 4	0.8837	0.9500	0.9157
Class 5	0.9545	0.7975	0.8690
Class 6	0.8607	0.9633	0.9091
Class 7	0.9429	0.8684	0.9041
Class 8	1.000	0.8571	0.9231
Class 9	0.6000	1.0000	0.7500

Depending on the confusion matrix and Table I, the accuracy of the UFO-GCN-SPANet model prediction is 0.9596, the average precision is 0.9205, the average recall is 0.9410, and the average F1 value is 0.9239. The results of the experimental data show that the UFO-GCN-SPANet model has superior prediction performance and high accuracy on this soil dataset.

Plot the Receiver Operating Characteristic Curve (ROC Curve, ROC Curve Plot) predicted by the model, as indicated in Fig. 8.

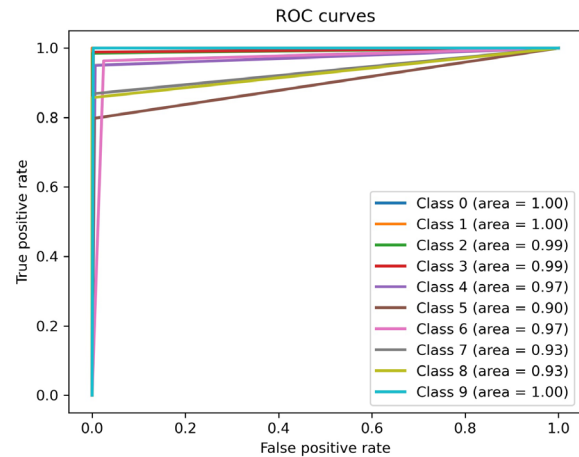


Fig. 8. ROC

As can be observed from Fig. 8, the area under the curve for each output category (Class 0 - Class 9) reaches 1.00 for Class 0, Class 1 and Class 9, with the lowest being Class 5, which is only 0.9, and above 0.9 for all other categories. It is shown that the prediction accuracy of each category is at a high level, indicating that the model predicts better.

2) Performance comparison experiments with other algorithms

The UFO-GCN-SPANet model was comparable to the more typical current models based on graph structure analysis, SAGEConv, GCNConv, GATConv, GraphConv, FeaStConv, ARMAConv, SGConv, GATv2Conv, TransformerConv, SSGConv, GENConv, and SuperGATConv were used for comparison experiments. The experimental results are given in Table II. As can be seen from Table II, in terms of the performance of prediction, the models based on graph structure processing all achieve better prediction results, with A_{cc} above 0.8, of which the GCNConv model has the lowest accuracy of 0.8562, and the GCN model optimised by introducing the unit forcing operation visual Transformer and the self-attention mechanism of the salient position (UFO-GCN-SPANet), the accuracy reaches 0.9596, an improvement of 12.07% compared to GCNConv. This significant improvement indicates that the prediction performance of the model can be effectively improved by the optimised UFO-GCN-SPANet model. In terms of P_{pv} , R_{ec} and $F1_Score$ values, the performance of most of the models is concentrated around 0.75, among which the GENConv and UFO-GCN-SPANet models are relatively outstanding, with all the three metrics reaching above 0.8. In particular, the UFO-GCN-SPANet model achieves 0.9205, 0.9410, and 0.9239 in P_{pv} , R_{ec} and $F1_Score$ values, respectively, which is an improvement of 27.88% in P_{pv} , R_{ec} and $F1_Score$ values compared to the lowest of the models, the GCNConv model, 33.26% and 30.29%. This result shows that the UFO-GCN-SPANet model is the optimal model among all the experimented models, which has a significant advantage in processing the data and is also reflected in the superiority in prediction accuracy.

TABLE II
PREDICTIVE PERFORMANCE INDICATORS OF THE MODELS

Class	A_{cc}	P_{pv}	R_{ec}	$F1_Score$
SAGEConv	0.8941	0.7597	0.7473	0.7504
GCNConv	0.8562	0.7198	0.7061	0.7091
GATConv	0.8764	0.7358	0.7329	0.7312
GraphConv	0.8752	0.7503	0.7080	0.7147
FeaStConv	0.8878	0.7537	0.7423	0.7466
ARMAConv	0.8777	0.7477	0.7336	0.7390
SGConv	0.8663	0.7492	0.7077	0.7196
GATv2Conv	0.8916	0.7745	0.7359	0.7494
TransformerConv	0.8916	0.7548	0.7626	0.7568
SSGConv	0.8840	0.7662	0.7398	0.7457
GENConv	0.9092	0.8872	0.7987	0.8210
SuperGATConv	0.8916	0.7570	0.7548	0.7553
UFO-GCN-SPANet	0.9596	0.9205	0.9410	0.9239

As evidenced in Table II, the proposed UFO-GCN-SPANet model achieves state-of-the-art performance across all evaluation metrics (Accuracy, Precision, Recall, F1-Score) compared to a wide range of established graph neural network

baselines. This significant performance advantage, exemplified by the 12.07% improvement in Accuracy over GCNConv and substantial leads over other strong contenders like GATConv and GraphConv, unequivocally validates the effectiveness of the overall architecture. This superior performance is directly attributable to the core innovations embedded within UFO-GCN-SPANet. The cascaded integration of these specifically designed components (UFO-ViT \rightarrow GCN \rightarrow SPANet) creates a synergistic effect. UFO-ViT lays the groundwork with efficient global understanding, GCN incorporates the spatial sensor topology, and SPANet performs targeted, context-aware refinement. This holistic design, prioritizing both predictive accuracy and operational efficiency, is the cornerstone of UFO-GCN-SPANet's success and represents its key novelty in addressing the practical demands of precision irrigation systems.

D. Ablation Study

To rigorously evaluate the contribution of each key innovative component in the proposed UFO-GCN-SPANet architecture, we conduct a comprehensive ablation study. We systematically remove or substitute core modules and evaluate the performance on the same soil moisture dataset. The variants compared are:

UFO-GCN-SPANet (Full Model): Our proposed complete architecture.

UFO-GCN: Replace UFO-ViT with a standard Transformer layer (using softmax attention).

GCN-SPANet: Replace SPANet with a standard multi-head self-attention layer.

GCN Only: Use only the GCN module as the core model.

The results of the ablation experiment are shown in Table III.

TABLE III
ABLATION STUDY RESULTS (PERFORMANCE ON TEST SET)

Model Variant	A_{cc}	P_{pv}	R_{ec}	$F1_Score$
GCN	0.8675	0.8698	0.8676	0.8625
UFO-GCN	0.8978	0.9034	0.8978	0.8969
GCN-SPANet	0.9294	0.9308	0.9294	0.9281
UFO-GCN-SPABlock	0.9584	0.9587	0.9584	0.9581

As can be seen from the experimental results in Table III, UFO-GCN-SPABlock performed the best, with indicators of 0.9584, 0.9587, 0.9584 and 0.9581, respectively, which were significantly better than other models, indicating that the proposed method had advantages in comprehensive performance and was the most accurate in classifying the overall data. UFO-GCN, which removing SPANet entirely results in a further performance degradation compared to the full model. This illustration suggests that SPANet's SPS algorithm is not just an alternative but a superior mechanism that offers significant performance gains and critical computational savings. The GCN Only baseline performs substantially worse than the full model and even the ablated variants containing attention, underscoring the necessity of incorporating sophisticated

global and contextual modeling. Adding UFO on top of GCN will increase all accuracy metrics compared to GCN, confirming that the linear complexity of UFO-ViT is critical to achieving high performance and practical efficiency in global feature extraction. The ablation study provides strong empirical evidence that the proposed UFO-ViT module and SPANet module (with its SPS algorithm), integrated in the specific cascaded order, are indispensable and synergistic innovations within the UFO-GCN-SPANet architecture. Each component contributes significantly to the model's final high accuracy and efficiency, justifying the novelty and design choices of the proposed framework.

E. Computational Efficiency and Performance Analysis

Experiments executed on consumer-grade hardware (MSI GL65 laptop, 32GB RAM). We compare the underlying algorithm GCN with the model we extracted from the total training time, Average CPU usage, Average memory usage, Average GPU usage, Average GPU memory usage and Best validation accuracy. The results of the ablation experiment are shown in the Table IV.

TABLE IV
COMPUTATIONAL EFFICIENCY AND PERFORMANCE ANALYSIS
OF THE PROPOSED MODEL

Evaluation indicators	GCN	Proposed Model	Delta
Total training time	218.62 s	558.57s	+339.95
Average CPU usage:	0.30%	1.25%	+0.95%
Average memory usage	52.50%	52.22%	-0.28%
Average GPU usage	11.99%	13.57%	+1.58%
Average GPU memory usage	14.06%	14.73%	+0.67%
Best validation accuracy	0.9168	0.9289	+1.21%

As can be seen from Table IV, the proposed UFO-GCN-SPBlock architecture achieves a notable accuracy improvement of 1.21% over the baseline GCN model, at the cost of a 2.6x increase in training time. Interestingly, we observed remarkably low hardware utilization rates (CPU ~1%, GPU ~13%) during training. This indicates that the current training pipeline is likely constrained by I/O bottlenecks (e.g., data loading and preprocessing) rather than the computational intensity of the model itself. This presents a significant opportunity for acceleration through pipeline optimization. Furthermore, the minimal change in GPU memory consumption (14.06% to 14.73%) suggests that our model's increased complexity is primarily computational, not parametric, making it a suitable candidate for memory-constrained edge deployment scenarios once the computational efficiency is improved.

VI. CONCLUSION AND DISCUSSION

Soil moisture content plays a major role in agricultural production and water management, and is directly related to crop growth and irrigation efficiency. Accurate prediction of soil water content enables scientific irrigation and optimization of

water resources. In tea tree precision irrigation, when making the decision of precision irrigation, farmers are not concerned about the specific soil water content data, but more concerned about whether the soil is in the degree of drought, moderate or over-wet state, and then dynamically adjust the amount of irrigation water according to the value of this degree. Therefore, changing the soil water content prediction problem into a classification problem and formulating an irrigation strategy based on the prediction results can achieve precision irrigation more effectively.

This manuscript proposes the innovative and efficient UFO-GCN-SPANet architecture for precise irrigation evaluation, with demonstrated compatibility for integration with IoT platforms using LoRaWAN, 4G/5G communication protocols and MODBUS sensor interfaces. The core novelty resides in three interconnected contributions:

The pioneering integration of UFO-ViT's linear-complexity self-attention ($O(N)$) for computationally efficient yet powerful global spatio-temporal feature extraction, directly overcoming the $O(N^2)$ bottleneck in standard approaches.

The introduction of SPANet with its novel Salient Position Selection (SPS) algorithm, which dynamically focuses computation on the most relevant contextual features, achieving significant gains in both predictive performance and computational/memory efficiency compared to standard attention mechanisms.

The design and validation of an optimal cascaded structure (UFO-ViT \rightarrow GCN \rightarrow SPANet) that sequentially leverages global context, spatial relationships, and focused refinement, specifically tailored to the efficiency and accuracy requirements of resource-constrained agricultural IoT applications. Extensive experiments and ablation studies confirm the substantial individual and synergistic value of each component. This work demonstrates that intelligent architectural design, featuring purpose-built efficient modules, is key to enabling high-performance AI solutions for real-world precision agriculture.

While the proposed UFO-GCN-SPANet demonstrates strong performance, several limitations should be acknowledged:

Sensor Data Quality. The model's accuracy may degrade with missing or noisy sensor inputs, particularly for soil conductivity measurements which showed $\pm 15\%$ variability in our field tests.

Environmental Factors. Extreme weather conditions (e.g., heavy rainfall >50 mm/day) may temporarily disrupt LoRa communications as shown in Fig. 2, requiring manual data imputation.

Crop Specificity. Current validation is limited to tea plants, though the architecture is theoretically adaptable to other crops.

Temporal Resolution. The 15-minute sampling interval may miss rapid moisture changes during irrigation events, suggesting future work should explore higher-frequency sensing.

System Integration. The proposed framework maintains compatibility with commercial IoT irrigation platforms through MODBUS sensor interfaces and OpenADR control outputs, though field deployment may require gateway-level protocol

adaptation, suggesting future work should develop plug-and-play middleware for heterogeneous systems.

Enhance practicality and scalability. This research can be undertaken in four primary dimensions. 1) Training Pipeline Optimization: We will eliminate the identified I/O bottleneck by implementing asynchronous data loading, prefetching, and on-GPU preprocessing to drastically reduce training overhead. 2) Large-Scale Validation: We will rigorously benchmark the model's scalability on massive sensor networks (>100,000 nodes) to assess real-world applicability. 3) Model Compression: Techniques like pruning and quantization will be explored to create lightweight variants for edge deployment. 4) Architectural Refinement: We will investigate more efficient attention mechanisms to reduce computational costs while preserving performance gains. These steps will directly address the trade-off between accuracy and efficiency, advancing the model toward practical agricultural implementation.

REFERENCES

- [1] A. Puspaningrum, A. Sumarudin and W.P. Putra. "Irrigation Prediction using Machine Learning in Precision Agriculture," in Proc. 5th International Conference of Computer and Informatics Engineering (IC2IE), Jakarta, Indonesia, 2022, pp. 204-208, doi: 10.1109/IC2IE56416.2022.9970092.
- [2] N.M. Priya, G. Amudha, M. Dhurgadevi, N. Malathi, K. Balakrishnan and M. Preetha. "IoT and Machine Learning based Precision Agriculture through the Integration of Wireless Sensor Networks," Journal of Electrical Systems, vol.20, no.4s, pp. 2292-2299, 2024. DOI: 10.52783/jes.2399
- [3] R. Filgueiras, T.S. Almeida, E.C. Mantovani, S.H.B. Dias, E. I Fernandes-Filho, F.F.da Cunha and L.P. Venancio. "Soil water content and actual evapotranspiration predictions using regression algorithms and remote sensing data," Agricultural Water Management, vol.241, pp.106346, 2020. DOI: 10.1016/j.agwat.2020.106346
- [4] E.A. Abioye, M.S.Z. Abidin, M.S.A. Mahmud, S. Buyamin, M.K.I. AbdRahman, A.O. Otuoze, M.S.A. Ramli and O.D. Ijike "IoT-based monitoring and data-driven modelling of drip irrigation system for mustard leaf cultivation experiment," Information Processing in Agriculture, vol.8, no.2, pp.270-283, 2021.DOI: 10.1016/j.inpa.2020.05.004
- [5] L.M. Narakala, A. Yadav, H. Upreti and G. Das Singhal. "Prediction of Crop Water Stress Index (CWSI) Using Machine Learning Algorithms," in Proc. World Environmental and Water Resources Congress, Milwaukee, Wisconsin, 2024, pp. 969-980. DOI: 10.1061/9780784485477.086
- [6] E. Bwambale, F.K. Abagale and G.K. Anornu. "Data-driven model predictive control for precision irrigation management," Smart Agricultural Technology, vol.3, pp.100074, 2023. DOI: 10.1016/j.atech.2022.100074
- [7] A. Bhoi, R.P. Nayak, S.K. Bhoi and S. Sethi. "Automated precision irrigation system using machine learning and IoT," in Proc. Intelligent Systems: Proceedings of ICMIB 2020, Singapore, 2021, pp.275-282. DOI: 10.1061/9780784485477.086
- [8] D.M.M. Vianny, A. John, S.K. Mohan, A.Sarlan, Adimoolam and A. Ahmadian. "Water optimization technique for precision irrigation system using IoT and machine learning," Sustainable Energy Technologies and Assessments, vol.52, pp.102307, 2022. DOI: 10.1016/j.seta.2022.102307
- [9] G.S. Campos N, A.R. Rocha, R. Gondim, T.L. Coelho da Silva and D.G. Gomes. "Smart & green: An internet-of-things framework for smart irrigation," Sensors, vol.20, no.1, pp.190,2019. DOI: 10.3390/s20010190
- [10] R. Liao, S. Zhang, X. Zhang, M. Wang, H. Wu and L. Zhangzhong. "Development of smart irrigation systems based on real-time soil moisture data in a greenhouse: Proof of concept," Agricultural Water Management, vol.245, pp.106632. 2021. DOI: <https://doi.org/10.1016/j.agwat.2020.106632>
- [11] Y.B. Choi and J.H. Shin. "Development of a transpiration model for precise irrigation control in tomato cultivation," Scientia Horticulture, vol. 267, pp. 109358, 2020. DOI: 10.1016/j.scienta.2020.109358
- [12] W.J. Jo and J.H. Shin. "Development of a transpiration model for precise tomato (*Solanum Lycopersicon L.*) irrigation control under various environmental conditions in greenhouse," Plant Physiology and Biochemistry, vol.162, pp. 388-394, 2021. DOI: 10.1016/j.plaphy.2021.03.005
- [13] M. Chen, Y. Sun, X. Cai, B. Liu and T. Ren. "Design and implementation of a novel precision irrigation robot based on an intelligent path planning algorithm," arXiv preprint, arXiv:2003.00676, 2020. DOI: 10.48550/arXiv.2003.00676
- [14] K. Wu, H. Desesquelles, R. Cockenpot, L. Guyard, V.Cuisiniez and S. Lambot. "Ground-penetrating radar full-wave inversion for soil moisture mapping in Trench-Hill potato fields for precise irrigation," Remote Sensing, vol.14, no.23, pp.6046, 2022. DOI: 10.3390/rs14236046
- [15] A. Abera, N.E.C Verhoest, S. Tilahun and J. Nyssen "Assessment of irrigation expansion and implications for water resources by using RS and GIS techniques in the Lake Tana Basin of Ethiopia," Environmental monitoring and assessment, vol.193, pp.1-17, 2021. DOI: 10.1007/s10661-020-08778-1
- [16] T.N. Kipf and M. Welling. "Semi-supervised classification with graph convolutional networks," arXiv preprint, arXiv:1609.02907, 2016.DOI: 10.48550/arXiv.1609.02907
- [17] M. Defferrard, X. Bresson and P. Vandergheynst. "Convolutional neural networks on graphs with fast localized spectral filtering," arXiv preprint arXiv:1606.09375, 2016. Doi: 10.48550/arXiv.1606.09375
- [18] J. Song. "Ufo-vit: High performance linear vision transformer without softmax," arXiv preprint, arXiv:2109.14382, 2021.DOI: 10.48550/arXiv.2109.14382
- [19] S.Fang, K. Li and Z. Li. "Salient positions based attention network for image classification," arXiv preprint, arXiv:2106.04996, 2021.DOI: 10.48550/arXiv.2106.04996
- [20] W.L. Hamilton, R. Ying and J. Leskovec. "Inductive representation learning on large graphs," arXiv preprint arXiv:1706.02216, 2017. Doi: 10.48550/arXiv.1706.02216
- [21] T.N. Kipf and M. Welling. "Semi-supervised classification with graph convolutional networks," arXiv preprint, arXiv:1609.02907, 2016. DOI: 10.48550/arXiv.1609.02907
- [22] P. Veličković, G. Cucurull, A. Casanova, A. Romero, P. Liò and Y. Bengio "Graph attention networks," arXiv preprint, arXiv:1710.10903, 2017. DOI: 10.48550/arXiv.1710.10903
- [23] C. Morris, M. Ritzert, M. Fey, W.L. Haniton, J.E. Lenssen, G.Rattan and M. Grohe. "Weisfeiler and Leman Go Neural: Higher-order Graph Neural Networks," arXiv preprint, arXiv:1810.02244, 2018. DOI: 10.1609/aaai.v33i01.33014602
- [24] N. Verma, E. Boyer and J.Verbeek. "FeaStNet: Feature-Steered Graph Convolutions for 3D Shape Analysis," arXiv preprint, arXiv:1706.05206, 2017. DOI: 10.48550/arXiv.1706.05206
- [25] F.M. Bianchi, D. Grattarola, L. Livi and C. Alippi. "Graph neural networks with convolutional arma filters," IEEE transactions on pattern analysis and machine intelligence, vol.44, no.7, pp.3496-3507, 2021. DOI: 10.1109/TPAMI.2021.3054830
- [26] F. Wu, A. Souza, T. Zhang, C. Fifty, T. Yu and K. Weinberger. "Simplifying Graph Convolutional Networks," arXiv preprint, arXiv:1902.07153, 2019. DOI: 10.48550/arXiv.1902.07153
- [27] S. Brody, U. Alon and E. Yahav. "How attentive are graph attention networks?," arXiv preprint, arXiv:2105.14491, 2021. DOI: 10.48550/arXiv.2105.14491
- [28] Y. Shi, Z. Huang, S. Feng, H. Zhong, W. Wang and Y. Sun. "Masked label prediction: Unified message passing model for semi-supervised classification," arXiv preprint, arXiv:2009.03509, 2020. DOI: 10.48550/arXiv.2009.03509
- [29] H. Zhu and P. Koniusz. "Simple spectral graph convolution," in proc. International Conference on Learning Representations (ICLR 2021), Vienna, Austria, 2021.
- [30] G. Li, C. Xiong, A. Thabet and B. Ghanem. "Deepergcn: All you need to train deeper gcns," arXiv preprint, arXiv:2006.07739, 2020. DOI: 10.48550/arXiv.2006.07739
- [31] D. Kim and Oh A. "How to find your friendly neighborhood: Graph attention design with self-supervision," arXiv preprint, arXiv:2204.04879, 2022. DOI: 10.48550/arXiv.2204.04879